AUTOIGNITION OF MONODISPERSE BIODIESEL AND DIESEL SPRAYS IN TURBULENT FLOWS

R. L. Gordon*,[1] and E. Mastorakos*
em257@eng.cam.ac.uk
*: Engineering Department, University of Cambridge, UK
1: Now at Rolls-Royce, Montreal, Canada

Abstract

A new experimental configuration has been developed for examining the effects of flow on the autoignition of dilute diesel and biodiesel sprays, where the spray is injected in the form of monodisperse individual droplets at right angles to a hot air turbulent flow. The ignition location has been measured by monitoring the OH* chemiluminescence. A qualitative comparison of the flame behaviour between ethanol, acetone, heptane and biodiesel as fuels has also been carried out. With decreasing volatility of the fuel, the flame showed progressively a higher number of individual droplets burning, with the first autoignition spots appearing at random locations but in general earlier than the intense droplet-flame emission. The time-averaged autoignition length increased with increasing air velocity and with increasing intensity of the turbulence, while it decreased with the temperature and the droplet size. The data can be used for validating models for two-phase turbulent combustion.

.

1. Introduction

The autoignition of liquid fuels in a turbulent environment is of significance to the operation of many combustion systems, particularly diesel engines, HCCI engines, and liquid fuel lean-burn gas turbines. Autoignition in non-premixed turbulent flows is a complex transient phenomenon that involves significant interactions between turbulence and chemical kinetics [1]. Experimental research into these phenomena in gaseous fuels has benefited from the use of generic burners where the source of the hot, turbulent oxidants has been decoupled from the combustion processes, enabling detailed parametric investigations [2, 3, 4, 5]. A natural development of these investigations is to examine the autoignition properties of liquid fuels, which is of more practical relevance.

Aggarwal [6] provides a review of the the work up to 1998 on spray combustion and ignition. There have also been recent investigations of fuel spray autoignition in a duct [7]. Droplet dispersion and evaporation of standard fuels and bio-fuels have been simulated in a turbulent cross-flowing stream [8], indicating that the droplet distribution, temperature and mass fraction were strongly dependent on the fuel type. Simulations of single droplet autoignition have shown the dominant physical parameter to be the gas temperature, with a minor dependence on droplet temperature, and the influence of droplet diameter being highly dependent on other ambient conditions [9]. Numerical simulation of sprays of different fuels [10] showed the impact of fuel type in ignition.

Single droplets have been investigated using microgravity experiments, which have identified multiple modes of droplet combustion including cool flame and two-stage ignition [11]. Hot flame ignition occurs above around 1000 K. The autoignition of kerosene droplets on a wire have also been investigated [12]. These works provide useful information on kinetics, but do not include information on the interaction between turbulence and autoignition.

This paper expands on earlier investigation into this burner that have been carried out for gaseous fuels [3,13] and aims to provide benchmark data . The experimental methods are described in Section 2, with Section 3 presenting the results and their discussion.

2. Methods

2.1 Experimental setup

This burner is a development of the confined turbulent hot co-flow burner that has been previously used to investigate gaseous autoignition [3]. A horizontal 600 mm long vacuum-jacketed quartz tube with inner diameter D of 31.8 mm was supplied with heated air by a bank of electrical air heaters (see Figure 1). Near the inlet of the tube was a 10 mm bore vertical opening to enable the installation of the droplet generator nozzle. For the experiments described here, the burner was operated over a bulk velocity range of 8.5–12.6 m/s, and a temperature range of 1030–1070 K. The co-ordinate system used in this work is axial distance z with z = 0 at the point of droplet injection, and radial distance r, with r = 0 at the center-line of the tube. A turbulence generating grid with blockage 45% and 2.5 mm holes was positioned at the inlet to the tube, 75 mm upstream of the injection port, for some of the data. Other turbulence generation grids, with holes of 5 mm and 2 mm, and blockage ratios for ranging from 55% to 45% were also used to examine directly the effects of turbulence on the autoignition processes. A flow straightener was positioned within the air supply tube, 500 mm (15 tube diameters) upstream of the turbulence grid. The air flow was controlled with a Bronkhorst mass flow control (MFC) meter. The heated air was maintained at a constant temperature by a feedback controller that maintained the flow temperature to within ±1 K of the reference temperature at operating temperature.

The fuel was supplied through a water-cooled nozzle fitted with an interchangeable sapphire orifice. The reservoir for the injector has a piezoelectric diaphragm which was supplied with a continuously variable square wave signal. As the fuel is injected through the orifice, the frequency of the diaphragm (ω) induces droplet breakup, enabling the generation of a chain of similarly sized individual droplets with diameters approximately 2–4 times that of the orifice, depending on ω. A 130 μm orifice was used for this work. Fuel was delivered to the nozzle at 2–3 bar via a syringe pump (IVAC P7000). Estimates of mass flow rates made from the droplet imaging were also made for every run.

2.2 Flow characterisation

Profiles of mean and RMS velocity and the longitudinal length scale, L_{11}, were measured with a DISA type 55M01/M10 standard bridge hot wire anemometer (HWA) with a 5 μm diameter, 1.25 mm long single-normal Type 55P16 platinum plated tungsten probe, run at 1.8 times overheat ratio. These velocity characteristics were sampled at 150 kHz. Integral length scales were calculated from the integral of the auto-correlation function of the velocity time signal up to the first zero crossing of the function. To achieve Reynolds number similarity with the hot flow, the velocity measurements were made at a cold mass flow rate that gives a Reynolds number of 3010, which is calculated for air at 1050 K, a diameter of 31.8 mm, and bulk velocity U_b =12.5 m/s.

Temperature characterisation was undertaken with a variety of thermocouples. An 850 μm bead R-Type thermocouple was used to take profile measurements at the nozzle injection plane, and also at the tube exit center-line to evaluate thermal losses. The temperature was also monitored at the center-line of the exit of the tube, with a consistent temperature loss of 35–45 K at z = 500 μm. A K-Type thin wire thermocouple (0.5 mm diameter) was positioned parallel to the flow extending from the center of the turbulence generating grid to

z = –5 mm. This was used as the main reference temperature for the experimental runs, and this, rather than the local mean temperature, is reported as the temperature parameter. Due to the experimental sensitivities associated with autoignition, detailed corrections were undertaken for both radiation and conduction, and the K- and R-thermocouples were calibrated against each other. The corrections were in the order of 45 K for the K-type and 15 K for the R-type.

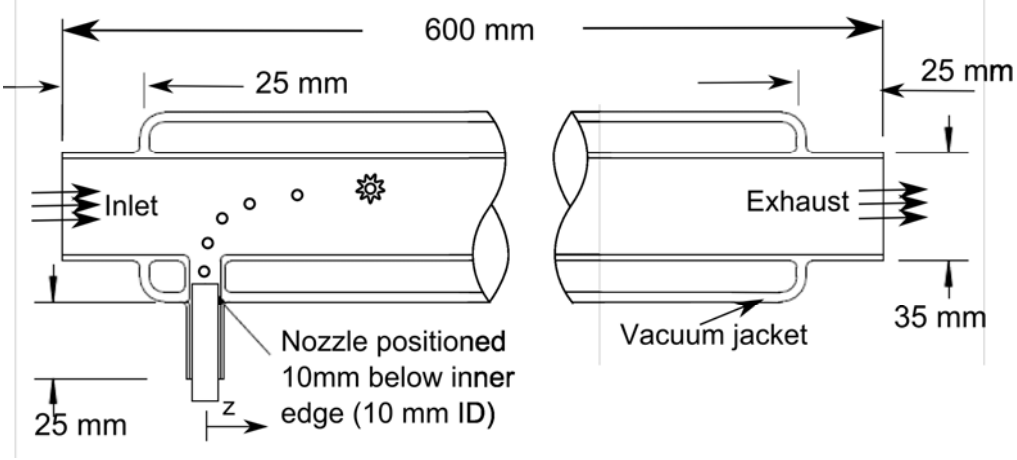

Figure 1: Flow schematic.

2.3 Imaging and emission spectra

A Phantom SA1.1 CMOS camera capable of 5.4 kHz at 1024×1024 resolution was used for droplet visualization. The droplet imaging was conducted with a diffuser and a bright light source, and imaged with a Micro Nikkor 60 mm lens at f # = 5.6 with a 13 mm extension ring. This gave a physical pixel resolution of 85 μm per pixel. Effective diameters were calculated from the droplet area, leading to a discretisation uncertainty in diameter of 5–10 % at droplet sizes around 500 μm. Exposure times of 1/20000 s and 1/10000 s give an image blur uncertainty of 25 μm and 50 μm near the inlet, respectively, in the direction of travel. Droplet imaging was performed at 5 kHz with 1/20000 s exposure time to generate approximate Probability Density Functions (PDF) of droplet size distribution.

A second SA1.1 was used with a state of the art Intensified Relay Optics (IRO) high-speed image intensifier and 310 nm band pass filter for OH* chemiluminescence imaging. The OH* chemiluminescence was imaged with a Cerco UV 100 lens at f # = 2.8 over a wide field of view (250 mm) with a 275 μm physical pixel resolution. Flame close-up sequences and long exposure with and without filters were also taken. Imaging was performed at 5 kHz.

Flame emission spectra were recorded at locations both up- and down-stream of the ignition location for the biodiesel experiments, and for one Diesel experiment. An Ocean Optics USB2000 spectrometer with a fiber optic coupled lens was used to collect the spectra. A 2" convex 100 mm focal length lens was used to integrate light from the ignition region onto the detector lens. Integration time was 1 s to maximise the signal. The spectra have been corrected for background, but not for spectral sensitivity of the detector.

3 Results and discussion

3.1 Flow characteristics

PDFs for Biodiesel are presented in Figure 2. Biodiesel provided the most mono-disperse droplets of all fuels tested, due to increased surface tension assisting clean droplet formation.

The small spike at 130 μm is due to a blemish on the optics that was not consistently removed during the image processing. Data taken 100 mm downstream of the injection location with biodiesel at 1700 Hz show no significant difference in the mean but a slight broadening of the PDF is apparent, which indicates that significant evaporation has not occurred by this stage.

The velocity profile across the tube is uniform to within ±10% of U_b, with a boundary layer about 2 mm growing along the walls. The r.m.s. of the streamwise turbulent fluctuations normalized by U_b was about 5% and 7.5%, while the integral lengthscale was about 1.5 mm and 2 mm for the 3 mm and 5 mm grids respectively. For a typical U_b=12 m/s, these estimates result in a turbulent eddy turnover time of 2.5 ms and 2.2 ms respectively.

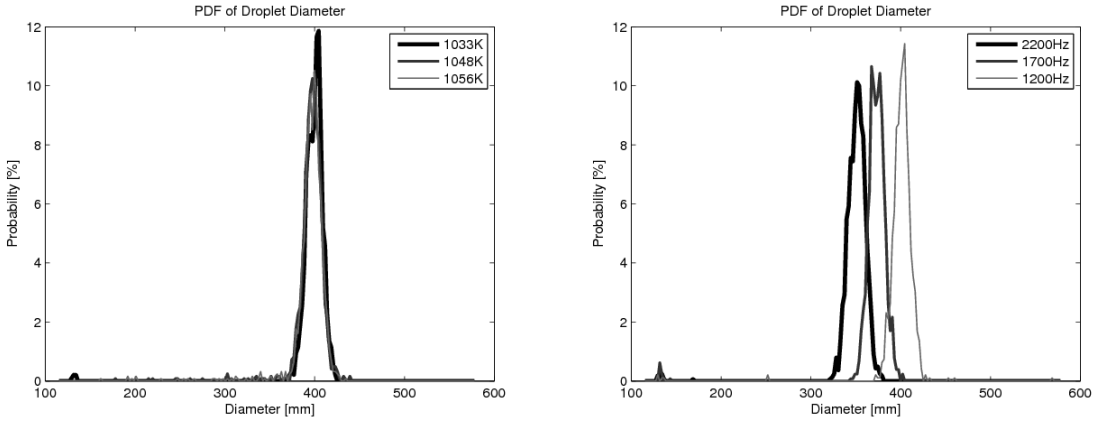

Figure 2: PDF of droplet diameter for biodiesel for ω =1700 Hz and U_b= 12 m/s (left) and for T = 1050 and U_b = 12 m/s (right). Data collected at z = 200 mm.

3.2 Autoignition lengths

The autoignition lengths of biodiesel for various U_b and turbulence grids are given in Fig. 3, while diesel is compared with biodiesel in Fig. 4. The lengths were determined by time-averaging the chemiluminescence movie and quantifying the location of the first rise. The following observations are made. First, for the same temperature, increasing U_b increases the autoignition length by a disproportionate amount (e.g. compare in Fig. 3 the data for 9.5 m/s with the data for 12 m/s). This implies a significant effect of the flow on the process. Second, for the same U_b, increasing the temperature decreases the autoignition length almost linearly. This almost linear trend implies a non-Arrhenius behaviour and is in contrast to the curved response of autoignition length *vs.* air temperature in the previous experiments with gaseous fuels (see [2,4,5] for methane jets in vitiated air and [3,13] for hydrogen and ethylene in this burner). This may be attributed to the different fuel vapour patterns in the present spray in cross-flow. Third, for the same T and U_b, a grid with larger holes delays autoignition. This is in excellent agreement with the similar finding from ethylene autoignition in hot co-flow [13] and is a trend also discussed at length in [1]: the smaller grid initially produces steeper mixture fraction gradients, but this also has the effect of producing earlier well-mixed spots which facilitates autoignition. Fourth, increasing the generator frequency at the same T and U_b gives a slightly earlier ignition, which may be expected due to the slightly smaller droplet diameters achieved when forcing at high firequencies (Fig. 2). Fifth, the good overall repeatability of the experiment is evident by comparing lengths measured with experimental campaigns when the temperature was increasing and when it was decreasing. Finally, diesel autoignites at a length about 10% longer than biodiesel.

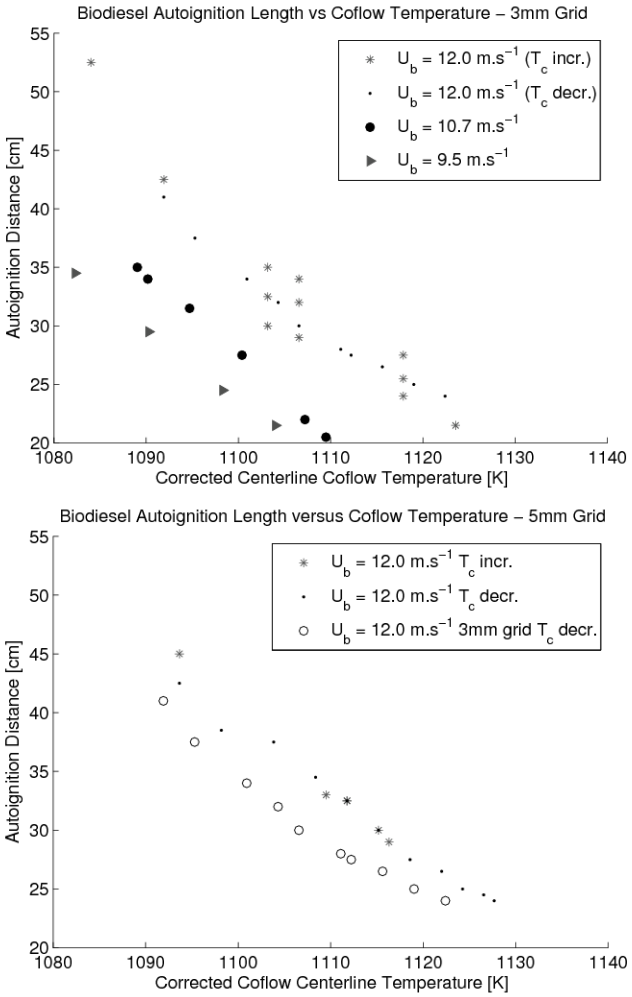

Figure 3: Biodiesel autoignition length *vs.* temperature for various U_b. Upper: 3 mm grid, $\omega = 1700$ Hz. For the 12 m/s case (stars), the three points at the same T correspond to 1200 Hz (top), 1700 Hz (middle) and 2200 Hz (bottom). Lower: 5 mm grid, 1700 Hz.

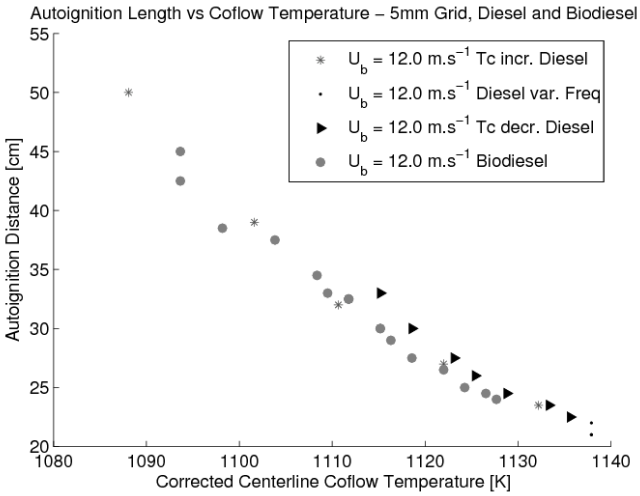

Figure 4: Biodiesel autoignition length for various U_b at $\omega = 1750$ Hz, 5 mm grid. At the highest temperature, the data points correspond to $\omega =$ 1250 Hz, 1750 Hz (top point, overlapping), and 2250 Hz (bottom).

3.3 Flame emission

Figure 5 shows the emission spectra from the biodiesel flames, with light collected over 1 s from various regions in the flame. Important emission lines have been marked, including, for example, OH* at 308 nm, CH*/CN* at 390 nm, CH* at 430 nm, and the C_2 Swan bands between 435 nm and 609 nm. It is evident that significant broadband emission occurs downstream of the ignition point, attributed to soot. The diesel flame shows the same peaks, but much higher broadband emission.

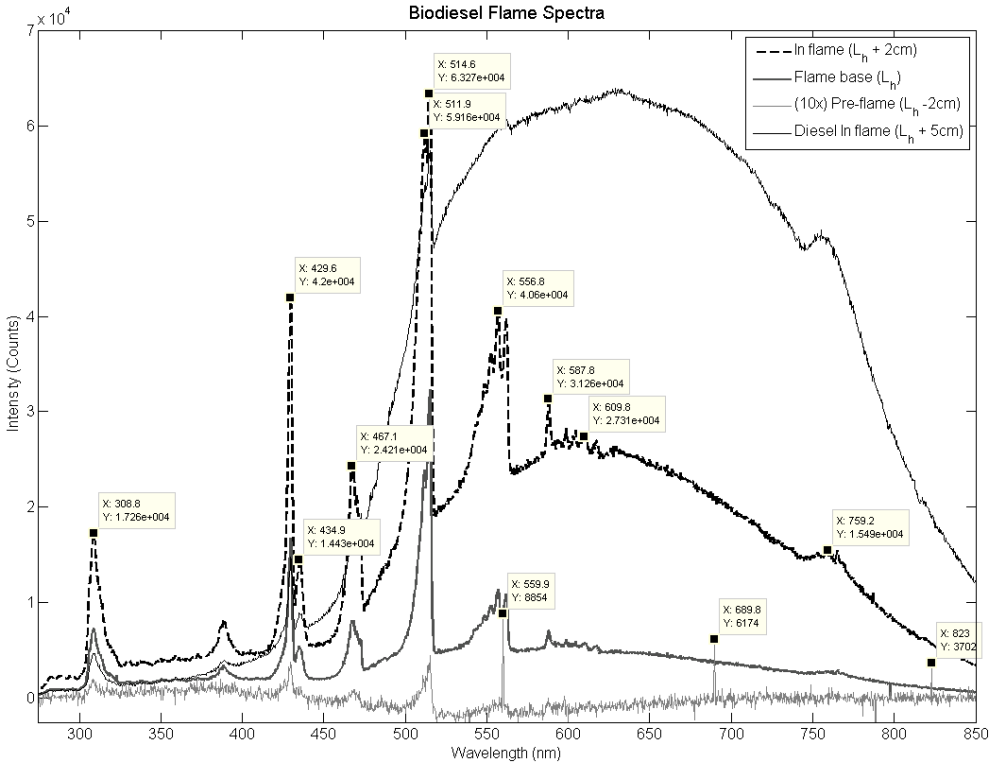

Figure 5: Emission spectra from biodiesel before, at, and after the ignition point and from diesel after the ignition point.

3.4 Ignition modes

The major part of this work focused on biodiesel, but other fuels have also been tested to examine qualitatively the effects of volatility. Figure 6 shows snapshots from high-speed chemiluminescence from experiments with ethanol, acetone, heptane, and biodiesel. The operating parameters (T, U_b) were chosen so that the ignition length was approximately similar for all fuels. The observations below do not depend on T, U_b, or ω.

The volatile fuels show diffuse chemiluminescence regions that emerge out of a dark background (characteristic of a new autoignition spot), with flamelets propagating around the spot and being convected with the mean flow. No individual droplet burning is evident. The behaviour of these two fuels is very similar to the gaseous fuels studied previously in this burner [3,13]. In contrast, the biodiesel shows mild light emission from a diffuse region, characteristic of vapour ignition, but also individual droplet trails that seem to ignite as they get close to already ignited vapour. The droplet trail lengths are consistent with our expectactions from the duration of the aperture opening of the camera and the bulk velocity, while the thickness of the trails are approximately 2-3 mm, corresponding to about 5 droplet

diameters. This is not far from our expectation for the size of a steady individual droplet flame. Heptane has an intermediate behaviour, with many diffuse vapour autoignition spots and droplet-scale flames.

An interesting behaviour is evident in Fig. 7. First, the emergence of individual autoignition spots is clear (see the growing emission to the left of the circle). Second, droplet-scale flames seem to collide and result either in a single flame or in a quenched region (see the evolution of the intense light points inside the circles). In (a), an individual droplet burning inside the circle is seen. It moves with the flow and, in image (b), two more droplet flames seem to have been developed upstream of it. The middle droplet flame evident in (c) eventually "collides" with the original at image (d), and at (e), it is not evident any more. This scenario is commonly observed. There is not sufficient information to understand exactly what is happening, but a hypothesis is that trails of vapour carried by the flow create conditions that are ripe for very fast flame propagation that catches-up with a droplet downstream of it. This causes the downstream droplet to be starved of oxygen and its flame then quenches. Note that for the size of the droplets of the present experiment, disappearance of the droplet due to their complete combustion is a much longer process than the residence time in the observed region of the burner, so this observation cannot be attributed to full consumption. Also, the spray is too dilute for droplet-droplet collisions.

4. Conclusions

Data have been presented for a monodisperse chain of liquid fuel droplets injected into a cross-flowing stream of heated turbulent air. Autoignition properties of biodiesel are investigated with respect to the effect of turbulence velocity fluctuations and length scale, droplet size, air velocity, and temperature. Increased turbulence intensity, achieved with the 5 mm grid, increased the ignition length. Increasing the air velocity and decreasing its temperature also increased the ignition length, while smaller droplet sizes reduced the ignition length. Diesel was found to ignite slightly later than biodiesel.

A qualitative investigation of the ignition modes of various fuels shows that fuel volatility significantly affects the nature of the ignition. Ethanol and acetone ignite entirely in the gaseous phase, whereas droplet ignition and combustion are found for heptane and biodiesel.

A systematic set of data exists from these experiments that is suitable for validation of CFD models for these processes.

Acknowledgements

Robert Gordon has been supported by the Royal Academy of Engineering – Royal Society Newton International Fellowship program. We thank Dr. Andrea Pastore for his assistance with the droplet generator.

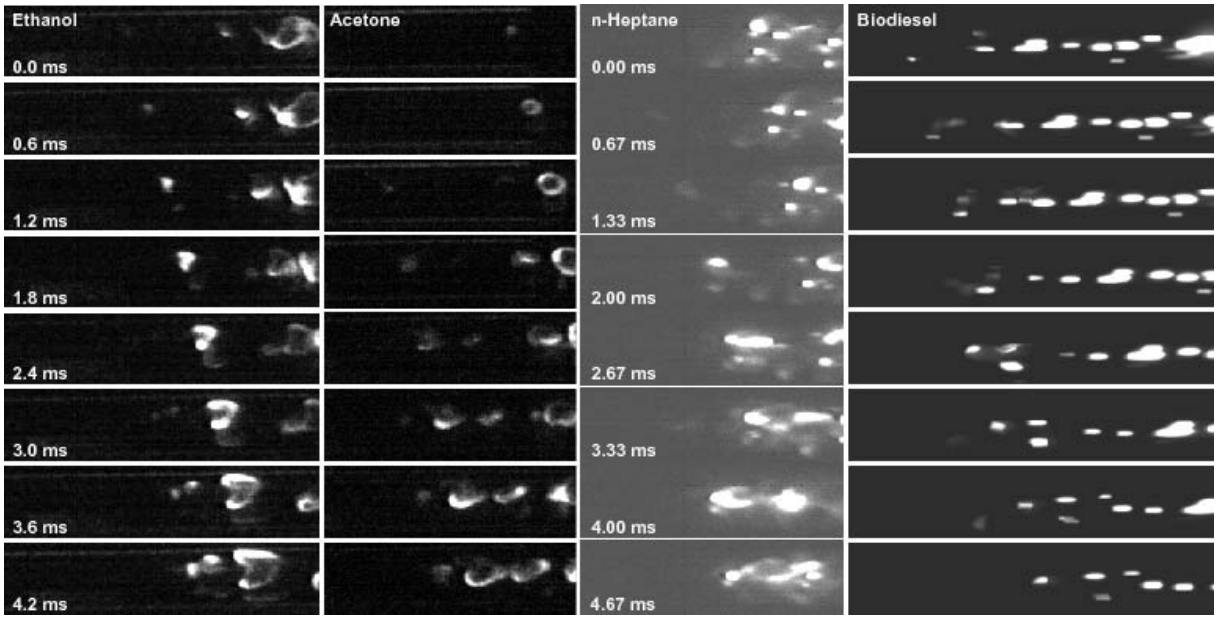

Figure 6: Temporal sequence from OH* chemiluminescence emission from various liquid fuels. The flow is from left to right, times for acetone are as for ethanol and for biodiesel as for heptane.

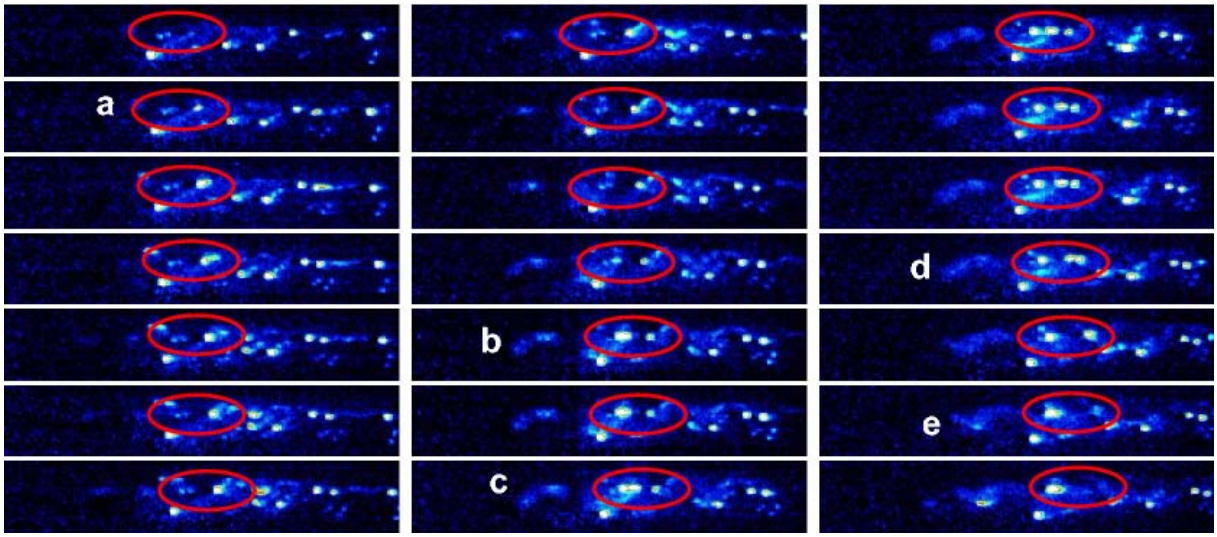

Figure 7: Sequence from an experiment with heptane, taken at 5000 frames per second. Time starts from the top left corner and continues down the first column, then down the second column, to finish at the lower right corner image. Flow from left to right.

References

[1] E. Mastorakos. Ignition of turbulent non-premixed flames. *Progress in Energy and Combustion Science*, 35:57–97, 2009.

[2] R. Cabra, J. Y. Chen, R.W. Dibble, A. N. Karpetis and R. S. Barlow. Lifted methane-air jet flames in a vitiated coflow. *Combustion and Flame*, 143(4):491–506, 2005.

[3] C.N. Markides and E. Mastorakos. An experimental study of hydrogen autoignition in a turbulent co-flow of heated air. *Proceedings of the Combustion Institute*, 30:883–891, 2005.

[4] R.L. Gordon, A.R. Masri and E. Mastorakos. Simultaneous Rayleigh temperature, OH- and CH_2O-LIF imaging of autoigniting methane flames issuing into a vitiated coflow. *Combustion and Flame*, 155:181–195, 2008.

[5] R.L. Gordon and A.R. Masri and E. Mastorakos. Heat Release Rate as Represented by [OH]x[CH_2O] and its Role in Autoignition. *Combustion Theory and Modelling*, 13:645–670, 2009.

[7] O. Hinkeldey, R. Koch, H.J. Bauer, M. Cano-Wolff and R. Schober. Laser based study of spray auto-ignition in a generic mixing duct. *Proceedings of the ASME Turbo Expo*, 3:37–46, 2008.

[6] S.K. Aggarwal. A review of spray ignition phenomena: Present status and future research. *Progress in Energy and Combustion Science*, 24(6):565–600, 1998.

[8] Barata, J. Modelling of biofuel droplets dispersion and evaporation. *Renewable Energy*, 33(4):769–779, 2008.

[9] R. Stauch, S. Lipp and U. Maas. Detailed numerical simulations of the autoignition of single n-heptane droplets in air. *Combustion and Flame*, 145(3):533–542, 2006.

[10] Gutheil, E. Numerical analysis of the autoignition of methanol, ethanol, n-heptane and n-octane sprays with detailed chemistry. *Combustion Science and Technology*, 105:265–278, 1995.

[11] S. Schnaubelt, O. Moriue, T. Coordes, C. Eigenbrod and H.J. Rath. Detailed numerical simulations of the multistage self-ignition process of n-heptane isolated droplets and their verification by comparison with microgravity experiments. *Proceedings of the Combustion Institute*, 28:953–960, 2000.

[12] Q.S. Khan, S.W. Baek and H. Ghassemi. On the autoignition and combustion characteristics of kerosene droplets at elevated pressure and temperature. *Combustion Science and Technology*, 179(12):2437–2451, 2007.

[13] C.N. Markides and E. Mastorakos. Experimental investigation of the effects of turbulence and mixing on autoignition chemistry. *Flow, Turbulence and Combustion*, 86:585–608, 2011.